physchem

MDPI

Review

Surface Coatings and Treatments for Controlled Hydrate Formation: A Mini Review

Tausif Altamash [1,*], José M. S. S. Esperança [2] and Mohammad Tariq [2,*]

[1] College of Health & Life Sciences, Hamad Bin Khalifa University, Education City, Qatar Foundation, Doha 34110, Qatar
[2] LAQV-REQUIMTE, Departamento de Química, Faculdade de Ciências e Tecnologia, Universidade NOVA de Lisboa, 2829-516 Caparica, Portugal; jmesp@fct.unl.pt
* Correspondence: tausif.altamash@gmail.com (T.A.); tariq@fct.unl.pt (M.T.)

Abstract: Gas hydrates (GHs) are known to pose serious flow assurance challenges for the oil and gas industry. Neverthless, over the last few decades, gas hydrates-based technology has been explored for various energy- and environmentally related applications. For both applications, a controlled formation of GHs is desired. Management of hydrate formation by allowing them to form within the pipelines in a controlled form over their complete mitigation is preferred. Moreover, environmental, benign, non-chemical methods to accelerate the rate of hydrate formation are in demand. This review focused on the progress made in the last decade on the use of various surface coatings and treatments to control the hydrate formation at atmospheric pressure and in realistic conditions of high pressure. It can be inferred that both surface chemistry (hydrophobicity/hydrophilicity) and surface morphology play a significant role in deciding the hydrate adhesion on a given surface.

Keywords: gas hydrates; flow assurance; hydrate adhesion; hydrate-phobic surfaces; wettability; coatings

check for updates

Citation: Altamash, T.; Esperança, J.M.S.S.; Tariq, M. Surface Coatings and Treatments for Controlled Hydrate Formation: A Mini Review. *Physchem* **2021**, *1*, 272–287. https://doi.org/10.3390/physchem1030021

Academic Editor: José Antonio Odriozola

Received: 29 October 2021
Accepted: 30 November 2021
Published: 4 December 2021

Publisher's Note: MDPI stays neutral with regard to jurisdictional claims in published maps and institutional affiliations.

Copyright: © 2021 by the authors. Licensee MDPI, Basel, Switzerland. This article is an open access article distributed under the terms and conditions of the Creative Commons Attribution (CC BY) license (https://creativecommons.org/licenses/by/4.0/).

1. Introduction

Gas hydrates (GHs) are ice-like crystalline solids made up of appropriate-size gas (guest) molecules (e.g., CH_4, C_3H_8, CO_2, N_2, H_2) entrapped within the polyhedral cavities formed by the hydrogen-bonded network of water (host) [1–3]. The van der Waals forces allow the small gas molecules to stabilize the host cages at low temperature and high pressures [4]. The size of the entrapped guest and the cavities influence the structure of a given gas hydrate unit, *viz.*, CH_4 and CO_2 form hydrates with cubic structure I (sI) and C_4H_{10} forms cubic structure II (sII) hydrates, whereas hexagonal structure H (sH)-type hydrates are formed by a mixture of hydrocarbons such as CH_4 and cyclopentane [5].

High-pressure and low-temperature conditions are often encountered during oil/gas exploration in deeper sea [6]. Since, some water is always available within the transmission pipelines, it provides suitable conditions for hydrates to form and plug the pipelines [7]. To avoid the formation of GHs during production, industries use costlier technologies including dehydration, insulation, depressurization, or the most viable option, chemical inhibitors' injection [8–10]. Although the chemical method is considered the most viable from an economic viewpoint, the injection of high doses of chemicals can affect the aquatic systems. The strict regulations proposed opened the platform for the search of low-dosage hydrate inhibitors that need to be injected in quantities as low as 1 wt.% compared to the 25 wt.% for conventional inhibitors [11,12]. However, strategies using low-dosage inhibitors are not yet economical, energy efficient, and environmentally friendly. Therefore, another method that is becoming popular these days is the use of hydrate-phobic surface treatment or coating that allows the hydrates to form but will not allow them to stick to the walls and form deposits, thus transporting the slurry out from the hydrate stability zone without hampering the production.

The formation of GHs is a crystallization step, where, first, the gas is dissolved in the aqueous phase at adequate temperature and pressure conditions. Once the aqueous phase is supersaturated, the nucleation occurs depending on the driving force (mainly subcooling or the initial pressure) followed by the hydrate crystals' growth until the system attains a steady state (when the maximum conversion of water to hydrates is reached) [13,14]. Homogeneous nucleation of hydrates is rarely observed, whereas nucleation that occurs in the presence of a foreign surface, known as heterogeneous nucleation, is more widespread since it is energetically favored [1]. Generally, gas hydrates grow at the gas/liquid interface and the importance of several aspects of the surface and interfacial phenomena involved in hydrate formation are documented in detail. For instance, Zerpa et al. [15] identified that, in the case of a hydrate-forming system in a closed vessel or a pipeline, many interfaces exist that are prone to hydrate formation and agglomeration: vapor/liquid, vapor/solid, liquid/solid, solid/solid, and liquid/liquid, where the vapor indicates the hydrate-forming gas, solid is pipeline, reactor wall, or hydrate surface, and liquid can be either water, oil, or condensate.

On one hand, GHs are a nuisance for the oil/gas industry, while, on the other, they can form/dissociate with ease and can accommodate a large quantity of gas, which opens many avenues for their usage in processes such as gas capture and storage, gas transportation, separation, refrigeration, and in desalination to name just a few [16–22]. Such applications require a rapid formation of hydrates. To accelerate the kinetics of formation, chemical or physical methods are generally used. Kumar et al. [23] reviewed the area of surfactants and concluded that the presence of a surfactant in the system reduces the interfacial tension between the vapor/liquid interface, which enhanced the mass transfer, resulting in more hydrate production. Linga and Clarke [24] summarized the role of reactor designs and physical methods such as sand packs, silica gels, dry water, foams, nano particles, and hydrogels, which may help to enhance the surface area that ultimately leads to enhanced rates of hydrate formation. Nanoparticles [25], Carbon-based materials [26] including graphene [27] and activated carbon [28] that provide large surface area and ample nucleation sites, which promote the kinetics of hydrate formation, have also been reported. On the other hand, Numerous studies are available in the literature where distinct surfaces [29–34] are used for this purpose. Metal-induced hydrate nucleation has also been reported recently [35,36]. However, the use of surface treatments or coatings to accelerate the hydrate formation is in its infancy.

Nguyen et al. [37] critically reviewed the role of functionalized solid surfaces (mainly particles) and a confined environment in controlling hydrate formation and the underlying mechanism. The authors concluded that open hydrophobic solids can promote the hydrate formation kinetics, whereas hydrophilic solids can reduce it. The mechanism proposed was that hydrophobic solids can order the structure of water and enhance the density of hydrate formers near the solid/liquid interface, whereas hydrophilic surfaces can distort the water structure and deplete the density of hydrate formers near the solid/liquid interface. The mechanism in the case of confined systems was found to be rather complex.

The area of smart coatings for controlled hydrate formation is relatively new and not yet reviewed. Wang et al. [38] dedicated just a small section in their review on coating technology for hydrate management. Manakov et al. [39] also presented briefly in their review the state of the art on the surface effect on hydrate nucleation. A survey of the literature until mid 2021 indicates that significant progress has been made at this front in the last decade that resulted in 16 published articles [40–55], 3 patents [56–58], and a few commercial products [59–62] already available in the market. Therefore, the aim of this work was to review the recent efforts made in the development of functionalized solid surfaces via coating or surface treatment and evaluating the role of the resulting solid/solid interactions in controlling hydrate nucleation and growth using model compounds such as tetrahydrofuran (THF) and cyclopentane (CP) at atmospheric pressure and gaseous molecules (CH_4, CO_2, etc.) in realistic conditions of high pressure. A list of the types of coatings, substrates used, hydrate-forming systems, and the P-T conditions in which the studies were carried out are summarized chronologically in Table 1.

Table 1. List of surface coatings or treatments, substrates, hydrate-forming substances, and conditions at which the tests were carried out to ascertain reduction or promotion in hydrate adhesion along with the respective references.

Hydrate Formers	Substrates	Coatings	Experimental Conditions	References
Tetrahydrofuran (19.1 wt.% in water)	-Clean glass -Bare steel	-l-Butanethiol, -1H, 1H, 2H, 2H-Perfluorodecane-thiol, -Methyl 3-mercaptopropionate, -4-Mercapto-l-butanol, -50/50 Butanethiol/methyl 3-mercaptopropionate, -50/50 Butanethiol/4-Mercapto-1-butanol, -Trichloro (1H, 1H, 2H, 2H perfluorooctyl) silane, -Octadecyl trichlorosilane, -80 wt.%/20 wt.% PEMA/fluorodecyl POSS	Atmospheric pressure, <4.4 °C	[40]
Cyclopentane (in water)	-Stainless steel (grade 309)	-Oleamide $(CH_3)(CH_2)_8(CH)_2(CH_2)_7CONH_2$; -Citric acid ester, based on $HOC(COOH)(CH_2COOH)_2$, -Nonanedithiol $HSCH_2(CH_2)_7CH_2SH$, -Commercial Rain-Xs (anti-wetting agent), -Graphite (based on planar sheets of carbon)	Atmospheric Pressure, T–n.a.	[41]
Tetrahydrofuran (19.0 wt.% in water)	-Steel -Silicone	-poly-divinyl benzene/poly(perfl uorodecylacrylate) (pDVB/pPFDA) Bilayer (BL) -linker free grafted coatings (LFG) with pPFDA thickness of 10 and 40 nm	Atmospheric Pressure, −15 °C	[42]
Cyclopentane (in water)	-Rough Steel -Flat Silicone	-pDVB/pPFDA (BL-LFG) with pPFDA thickness of 10 and 40 nm	Atmospheric Pressure, −15 °C	[43]
Methane (in water and water + LDHIs)	-Stainless steel crystallizer	-perfluoroalkoxy alkane polymer from DuPont Teflon coating, Cantech Precision Coatings Inc. (PFA)	41 bar, 6 °C	[44]
Tetrahydrofuran (1:15)	-Glass test tubes (Heavy wall borosilicate)	-(3-aminopropyl)triethoxysilane (APTES) -*N*-[3-(trimethoxysilyl)propyl]-ethylenediamine (AEAPTMS) with succinic acid (SA) linker to a glycerol at 1- or 2-position.	Atmoshperic Pressure, 0 °C	[45]
Cyclopentane (in water)	-Silicon	-octadecyltricholorosilane (OTS) -tridecafluoro-1,1,2,2 tetrahydrooctyl trichlorosilane (FS)	Atmospheric Pressure, −5 °C	[46]
Cyclopentane (in water) & Methane (74.7 mol%) + Ethane (25.3 mol%)	-Carbon Steel (Pristine & corroded)	-Omniphobic -Superhydrophobic	Atmopsheric Pressure, 500 psig and 1 °C	[47]
Tetrahydrofuran & Methane	-Carbon Steel	-A green fluorinated ethylene propylene (FEP) -A blue polytetrafluoro ethylene (PTFE) -B black polytetrafluoro ethylene (PTFE) -B green fluorinated ethylene propylene (FEP)	Conditions n.a.	[48]
Cyclopentane	-Silicon -Steel	-poly-divinylbenzene (pDVB)/poly-perfluorodecylacrylate (pPFDA) bilayer covalently bonded and grafted to substrates using iCVD process.	Atmospheric Pressure, −15 and 5 °C	[49]
Methane (74.7 mol%) + Ethane (25.3 mol%)	-Stainless Steel	-Omniphobic -Superomniphobic	1000 psig and 2.5 °C	[50]
Methane	-Glass -Steel 316 L	-ethyltriethoxysilane (ES) -*n*-dodecyltriethoxysilane (DS) -*n*-octyltriethoxysilane (OE)	4 °C, 100 bar (stationary experiments) and 150 bar (transient experiments)	[55]
Tetrahydrofuran (19.1 wt.% in water)	-Neodymium Magnet	-Ferrofluid (Iron oxide/magnetite 8% *v*/*v*, oil-soluble dispersant 14% *v*/*v*, light hydrocarbon oil 78% *v*/*v*)	Atmospheric Pressure, −5 °C; Mechanical tests for adhesion were performed at −15 °C	[51]

Table 1. *Cont.*

Hydrate Formers	Substrates	Coatings	Experimental Conditions	References
Tetrahydrofuran (19.0 wt.% in water) & Methane	-X70 pipeline steel -X80 pipeline steel -Zirconia (ZrO_2) -Tin plate	-Fluoro-coating (F-coating) -Polydimethylsiloxane (PDMS) -Hexagonal boron nitride (HBN) -Hydrophobic fuming SiO_2 (HB-630, diameter $\leq$ 300 nm)	Atmospheric Pressure, −3 °C; −10 °C, 8.2 MPa	[52]
Cyclopentane	-X90 pipeline steel	-Copper oxide (CuO) layer modified with Stearic acid	Atmospheric pressure, 1 °C	[53]
Cyclopentane	-X80 pipeline steel	-Cerium oxide (CeO_2)/polydopamine (pDA)	Atmospheric pressure, n.a. (0 °C > T > 7.7 °C)	[54]

2. Hydrate Adhesion and Deposition

It was envisaged from several works that hydrate deposition occurs at the pipeline wall. One study [63] suggested that if sufficient water is available, the hydrate particles will start growing either in the liquid phase or on a suitable seed present in the liquid phase, close to the gas/liquid interface, or at the pipeline wall. In another study [64] it was found that hydrate agglomeration was less profound compared to the stickiness between hydrate particles, hydrate particles to the wall, or a combination of the two effects. They suggested that wettability of the pipeline wall plays an important role in determining the stickiness of the hydrate particles, which are hydrophilic in nature. In the case of a hydrophobic surface, the formation of a water bridge can be reduced, which may influence the hydrate nucleation and deposition.

Later, Nicholas et al. [65] investigated the possibility of hydrate deposition on pipeline walls since it is the coldest point in the system and contains nucleation sites. A micromechanical force (MMF) apparatus was used to measure the strength of adhesion force of cyclopentane (CP) hydrate to a carbon steel substrate. The micromechanical force (MMF) measurement is a central technique that has been used to measure the strength of adhesive forces between the solid substrate samples and the hydrate particles in a majority of the works presented in this review. The working principal of the MMF apparatus is presented briefly in Figure 1, which can be consulted in detail elsewhere [65–68]. It was found that the adhesion forces between the hydrate-hydrate particles were higher than the forces between the hydrate and carbon steel in a water-free environment. It was proposed that capillary forces between hydrate and steel were dominating but not enough for the hydrates to deposit on the wall.

Aman and Koh [69] critically scrutinized the research revolving around various interfacial phenomena involved in gas hydrates' systems and pointed out that solid/solid interfacial behavior, especially adhesion of hydrate to the pipeline wall, is a crucial factor in flow assurance. This idea was later experimentally corroborated [70] and the need to address this issue using chemical and physical methods has been emphasized.

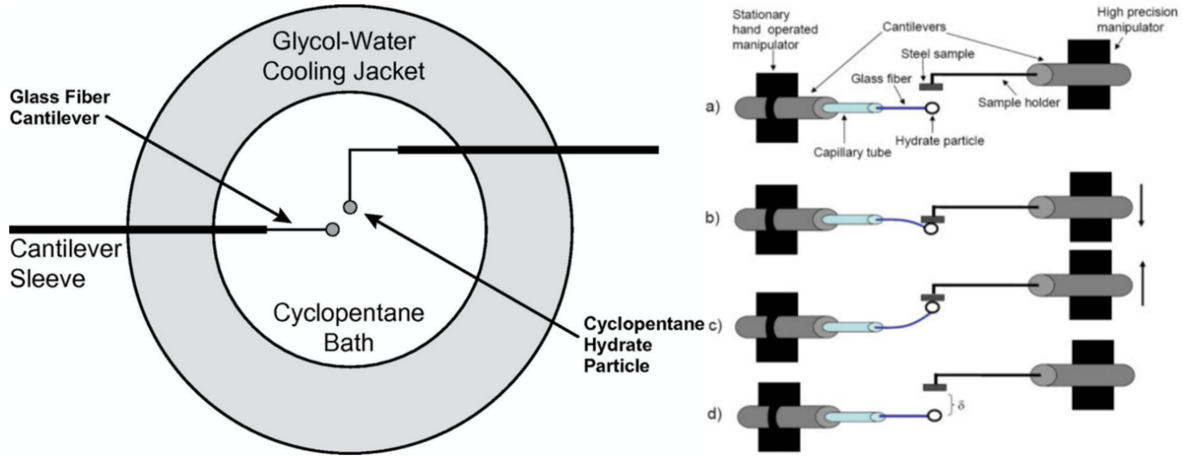

Figure 1. (**Left**) Schematic diagram of the top view of a cell of the micromechanical force (MMF) apparatus. (**Right**) Working mechanism of the MMF: The cantilever placed at the left is hand operated and holds the hydrate particle, whereas the right-hand one, where the solid substrate is placed, is highly precise. (**a**) Initial position of the cantilevers. (**b**) By moving down the precise cantilever, a preload can be applied to the hydrate particle, (**c**) the precise cantilever can be moved back until the particle is removed from the solid surface, and (**d**) the required distance (δ) to remove the particle from the solid sample can be registered. Following Hook's law, the distance is multiplied to the spring constant of the cantilever to obtain the force of adhesion. Reprinted with permission from ref. [68]. © 2021 Elsevier (**left**) and reprinted with permission from ref. [65]. © 2021 Elsevier (**right**).

3. Hydrate-Phobic Surface Treatments and Coatings

Various coatings and surface treatments were reported to alter the hydrate adhesion to solid surfaces [40–55]. We collected those works and categorized them into the following subsections for the ease of the reader.

3.1. Functionalized Hydrate-Phobic Surfaces

Smith et al. [40] reported that by functionalizing the solid surfaces systematically (varying hydrophobicity), the adhesion between the hydrates and the solid surfaces can be reduced. This will not allow the hydrate to deposit on the pipeline wall, which may lead to hydrate plug formation. This study was carried out using THF as hydrate former at atmospheric pressure and was the first of its kind where the role of surface energy and wettability on the adhesion force of hydrate particles in solid/solid contact were measured. The authors used glass/steel substrates and several functionalized coatings (Table 1). They demonstrated that treated surfaces compared to bare steel can reduce the adhesion strength of THF hydrates by a factor of four (Figure 2A). Such reduction is possible on low Lewis acid/base and van der Waals characterized surfaces.

Later, Aman et al. [41] studied, using a MMF apparatus, the adhesive forces between the cyclopentane hydrates and five distinctly modified steel surfaces in both dry (solid/solid) and water-wet (solid/liquid) conditions. The graphite-functionalized surface reduced the solid/solid adhesion force by 79% compared to the untreated steel surface due to a reduction in surface wettability, proved by contact angle measurements. Citric acid ester functionalization not only reduced the adhesive force by 98% but was also responsible for morphological changes in crystals that resulted in hydrate growth. However, the effectiveness of both surfaces decreased in water-wet conditions due to 7% and 55% reductions in adhesive forces, respectively. Nonanedithiol modification resulted in a 49% increase in adhesive forces due to the formation of specific cylindrical morphology at the hydrate (solid)/surface (solid) interface. Interfacial studies indicated qualitatively that citric acid ester adsorbed at the hydrate/steel interface easily since hydratephilic molecules may adsorb preferentially at the hydrogen bonding sites on the hydrate surface as observed by the adsorption isotherms for water/oil and hydrate/oil interfaces.

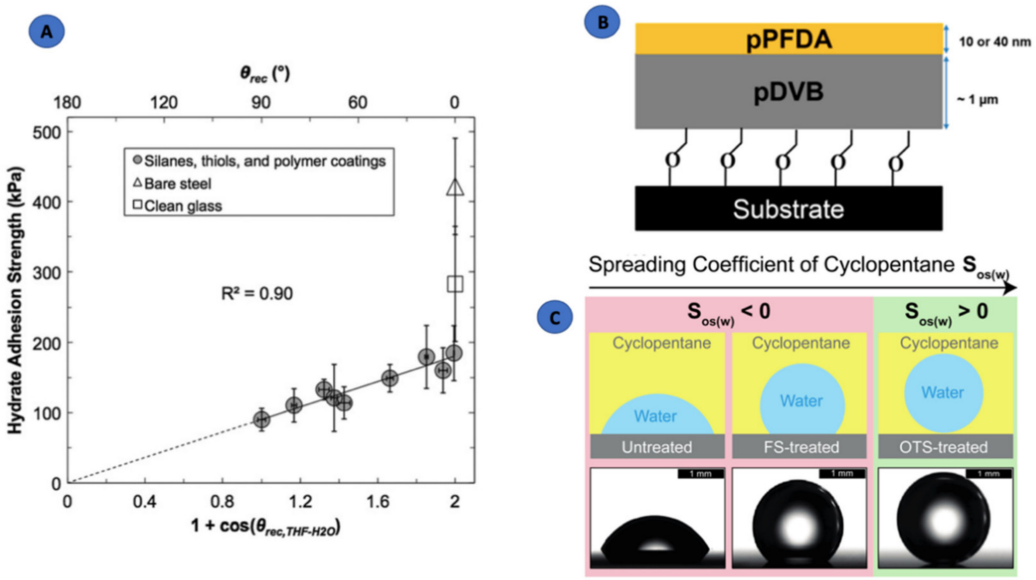

Figure 2. (**A**) Correlation between hydrate adhesion strength with the practical work of adhesion evaluated using the 19.1 wt.% THF in water solution on various functionalized surfaces. (**B**) A linker-grafted pPFDA/pDVB polymeric ice-phobic, hydrate-phobic, and hydrophobic coating. (**C**) Representation of water contact angles on solid surfaces (s), indicating two zones of spreading coefficient, $S_{os(w)}$ of cyclopentane (o) in presence of water (w). (**A**) Reprinted with permission from ref. [40]. ©2012 Royal Society of Chemistry. (**B**) Reprinted with permission from ref. [43]. ©2015 American Chemical Society.and (**C**) Reprinted with permission from ref. [46]. ©2017 American Chemical Society.

Hall and Baures [45] functionalized the glass test tube with glycerol in different configurations and tested their effects compared to polyvinylpyrrolidone (PVP) on THF hydrate nucleation. The conjugation of glycerol on the glass surfaces was achieved in different configurations: (1) through employment of two distinct silane spacers, (2) by attaching to glycerol at the 1 or 2 position covalently, and (3) by attaching a succinic acid spacer. Contact angle measurements were used to ascertain the desired functionalization of the surface. Induction times were measured for 1:15 THF solutions at 0 °C, and at least 50 data points were gathered on each modified surface. Among all the functionalized surfaces, the best hydrate inhibition results were shown by the surface modified by APTES and glycerol coupled at the 1 position (leaving a free 1,2-diol). Other modifications using AEAPTMS coupled with glycerol at the 1 or 2 position did not show any significant change compared to unmodified glass tubes. However, the test tube modified with APTES and succinic acid enhanced the THF hydrate formation.

Das et al. [46] treated the smooth and textured silicone surfaces with octadecyltricholorosilane (OTS) or tridecafluoro-1,1,2,2 tetrahydrooctyl trichlorosilane (FS) in order to design passive hydrate-phobic surfaces and measured the cyclopentane hydrate adhesion and accumulation on them. Among the silane-modified surfaces, the one treated with OTS exhibited almost null hydrate adhesive strength and lower accumulation. Although the FS-modified surfaces exhibited low surface energies, one useful parameter that was taken into account in this work was the measurement of contact angle hysteresis, i.e., the difference between the advancing and receding angles that provides information on the interaction between the liquid and solid surface under scrutiny. A large hysteresis indicates a larger pinning and higher roll-off angles. For instance, the untreated silicon surfaces in cyclopentane showed a ~24° hysteresis for water; this value was ~55° for FS-treated ones and was much lower for OTS-treated surfaces compared to other two. This indicates that the water droplet will stick to the untreated and FS-treated ones even at a tilt angle of 90°, whereas on OTS-treated surfaces, it will roll down just at an inclination of 2°. Another interesting aspect of this work was to study the spreading of the cyclopentane barrier film between the hydrate and solid surfaces. The spreading coefficients were measured, which

gave information about the relative spread of this interfacial film and its effect on hydrate adhesion (Figure 2C). The role of surface chemistry and texture plays a significant role in the spreading of such films. Although the surface energy criteria were found consistent in predicting the poor performance of untreated silicon, the spreading coefficient captured a complete picture of the performance for all the studied systems. In the case of a positive spreading coefficient for cyclopentane, the solid/water contact area reduced drastically due to the formation of a barrier film by cyclopentane that exhibited much lower hydrate accumulation and adhesion. OTS-coated samples resulted in almost negligible accumulation and a 2-fold reduction in adhesion compared to the FS-coated surfaces.

3.2. Polymeric Coatings

Sojoudi et al. [42] demonstrated using a chemical vapor deposition (CVD) method that hydrate-phobic bilayer polymeric coatings pDVB/pPFDA of varied thickness on steel and silicon surfaces can lead to a reduction in the ice and hydrate adhesion strength (Figure 2B). Bilayer polymer coatings of a highly dense, crosslinked network on top of a steel substrate covered with a 40-nm, fluorine-rich polymer film exhibited a 10-fold reduction in the hydrate adhesion strength. A significant substrate effect was observed through changes in the roughness values of the polymer films. The roughness in the case of the steel substrate was higher compared to silicon. Similarly, a slight difference in the contact angles was also observed due to increased fluorine concentration and different crystallinity of the 40-nm-thick films compared to the 10-nm one. The authors scanned a wide concentration (0–70 wt.%) of THF solutions and proposed that 19 wt.% should be used as a probe liquid. No statistically significant effect of subcooling and time on the adhesive behavior was observed since the adhesion strengths were comparable irrespective of their formation conditions. After a freezing/hydrate deposition and de-adhesion cycle, the coatings remained functional. However, their long-term durability in aqueous media and humid conditions needs to be explored.

These polymeric coatings were also tested for reducing the adhesion strength of ice and cyclopentane (CP) hydrates [43], another widely used model compound for studying natural gas hydrates at atmospheric pressure. The results were similar to what had been observed in the case of THF hydrates. The coated surfaces showed more than a 6-fold reduction in ice and 10-fold reduction in hydrate adhesion strength compared to bare steel and silicone surfaces. The durability of these coatings was assessed through sand erosion tests and repeated adhesion/de-adhesion cycles. The cost associated with the fabrication of these polymeric coatings is low due to the usage of low-cost polymer pDVB beneath a thin layer of pPFDA. The authors claimed that these covalently grafted polymeric coatings possessing the ice-phobic and hydrate-phobic as well as hydrophobic characters will be potential candidates for several industrial applications.

Sojoudi et al. [49] once again reported a detailed study on some mechanically robust hydrate and icephobic polymeric coatings that can be stable in harsh subsea or arctic environments with high pressures and low temperatures. They used initiated chemical vapor deposition (iCVD) method to apply rough polymeric films having a bilayer of poly-divinylbenzene (pDVB)/poly-perfluorodecylacrylate (pPFDA) on commercial silicon and steel substrates, showing a water contact angle above 150°. Surface roughness of the films was recorded as 178 and 313 nm on silicon and steel substrate, respectively, measured using optical profilometer. After application of the coatings on a rough steel surface, a six-fold reduction in the adhesion strength of the ice and a 10-fold reduction in cyclopentane hydrates' adhesion was observed. Sand erosion, nanoindentation, and nano-scratch tests and multiple adhesion/de-adhesion cycles ensured the robustness and durability of the developed coatings given the fact that they are covalently attached to the substrate surface.

The first report where hydrate-phobic coatings were tested in realistic conditions of high pressure was published by Perfeldt et al. [44]. The authors not only assessed the effect of hydrophobic coatings on the methane hydrate formation but also reported that the usage of such coatings can also help to cut down the concentration of LDHIs significantly. They

carried out the tests in separate stainless-steel crystallizers made up of non-coated and coated with hydrophobic perfluoroalkoxy alkane polymer (PFA). The interiors of the crystallizer including baffle, lid, impeller, and thermocouple were also coated with ~1000-mm PFA film except the shaft. The tests were carried out under low driving force (subcooling) and the induction time in the coated system was considerably higher compared to the uncoated system for reference solution. In the presence of inhibitors in a coated system, the nucleation rate was very low; thus, it was difficult to distinguish the temperature and pressure changes due to nucleation. The coated system also performed very well in reducing the hydrate growth. The coated system with just 0.02 wt.% LuvicapBio reduced the hydrate growth, equivalent to an uncoated system with 0.20 wt.% LuvicapBio.

Di Lullo et al. [48] characterized several commercial surface coatings that can be used to avoid hydrate adhesion to a pipeline wall for their roughness, contact angles (water and diiodomethane), and THF hydrate adhesion force measurements. The authors pointed out that the tests performed on model systems at atmospheric pressure may lead to erroneous conclusions. Therefore, a novel experimental methodology was proposed to truly assess the efficiency of this technology in realistic conditions of high pressure. The authors carried out two distinct adhesion tests with a H_2O: THF solution at atmospheric pressure and with a natural gas system at high pressures. Two commercial polymeric coatings produced by two different manufacturers, namely, polytetrafluoroethylene (PTFE) and fluorinated ethylene propylene (FEP), were applied on a carbon steel substrate to assess their effectiveness in hydrate inhibition. Hydrophobicity and oleophobicity of the surfaces under study were assessed by measuring water and diiodomethane contact angles, respectively. The authors made five repetitions of adhesion measurements in the case of the THF systems. They faced partial hydrate detachment and out-of-range issues while measuring adhesion on carbon steel and B samples; therefore, those results were not reported. Tests performed on methane hydrates in autoclave were repeated thrice for each system. The results of the performance of both the commercial coatings from both the methods were compared, indicating that the THF method can underestimate their performance in comparison to the test performed in realistic conditions of high pressure, which may lead to erroneous rankings. However, the authors did not provide the temperature and pressure conditions at which the experiments were carried out and paid attention to the fact that the hydrates formed by THF (type sII) and methane (type sI) presented distinct structures.

3.3. Superhydrophobic and Omniphobic Coatings

Brown et al. [47] presented two low-adhesion protective coatings, a superhydrophobic anti-icing coating and an omniphobic corrosion-resistant coating, and determined their efficiency in reducing the hydrate adhesion on pristine and pre-corroded carbon steel surfaces. Cyclopentane and the methane/ethane mixture both formed sII hydrate structure and were used for testing the effect of both the coatings at atmospheric, high-pressure, and dynamic conditions using a micromechanical adhesion force measurement apparatus and a rocking cell assembly. The MMF experiments performed at atmospheric and high-pressure conditions indicated that the application of the coating resulted in a reduction of adhesive forces between hydrate and solid carbon steel surfaces, more so in the case of the corroded steel. Rocking cell tests indicated that at low-water content the hydrate deposition time reduced significantly. The omniphobic and superhydrophobic coatings decreased the adhesion force by 53% and 29%, respectively, on a pristine surface, whereas the decrease on pre-corroded surfaces was found to be 96% and 95%, respectively. Rocking cell experiments conducted at high pressure indicated that hydrate deposition could be delayed up to 24 h using coated surfaces in a low-water content system.

Later, Pickarts et al. [50], in order to develop a readily applicable robust strategy to reduce the deposition behaviour of various solids (hydrates, wax, asphaltene) within the pipeline, carried out extensive testing of polymeric omniphobic and superomniphobic surface material formulations at atmospheric and high-pressure conditions. Different experimental setups were used to unravel the interactions between the coatings with

water, gas hydrate, asphaltene, and crude oil. At atmospheric pressure, on a corroded surface, the omniphobic surface treatment enhanced the water contact angle from 0° to 91.5°. The low surface energy and water-repellent properties of omniphobic material made the authors test it for its anti-hydrate properties. Compatibility tests were carried out by applying the omniphobic formulation on both sides of the piece of substrate and submerging it into various chemicals representing the substances that might be present in production lines such as kerosene, xylene, and jet propulsion fuel 8 (JP8) for 120 days. The samples were regularly checked for any change in appearance, weight, and adhesion. No detectable changes were noticed, even after 4 months of submersion in the case of kerosene and JP8. However, slight changes in the surface colour were noticed in the case of xylene. Adhesion and weight remained unaltered in all cases. High-pressure measurements were performed using a rocking cell apparatus where the treated/untreated stainless-steel substrates were placed at the bottom of the experimental chambers after filling the desired liquid phase (model oil/water). An isochoric-isothermal method coupled with shear-induced conditions was used to assess the hydrate inhibition ability of the formulation and indicated that the surface treatments inhibit the hydrate deposition for up to 3 days with good repeatability. Omniphobic treatments were also found effective compared to untreated/superomniphobic treatments in reducing the deposition of asphaltene and crude oil on its surface. The authors are looking to scale up the selected formulation and testing in a high-pressure flowloop to produce a robust surface treatment that can be recommended to industries as a strategy to manage solid deposition within the pipelines.

Dong et al. [53] created a superhydrophobic (water and hydrate repellent) coating of CuO on the surface of X90 pipeline steel by electrodeposition and hydrothermal treatment of Cu followed by surface modification using stearic acid. The microstructure of the modified surface looks like the structure of a lotus leaf, indicating potential super hydrophobicity. Later, the water contact angles on the modified surface in air and cyclopentane were found to be 160° and 170.7° compared to 51° and 93° on bare X90 steel. The prepared surface turned the water droplets spherical when dropped on it. Just by tilting the surface at 5.7° and 2.4° in air and cyclopentane, respectively, the droplets can be rolled off from this surface immediately. Morphological analysis indicated that the hydrate particles formed spherical morphology, resulting in the reduction of the interfacial contact area and hydrate adhesion force to the solid surface. It was found during the hydrate detachment tests that a force of 0.0016 N was not enough to remove the hydrate particle from bare X90 steel, whereas from the superhydrophobic surface it can be removed by just applying a force of 0.00013 N.

More recently, in a similar work, Zhang et al. [54] reported the preparation of a bio-inspired superhydrophobic coating using a static self-assembly method. Inorganic material of high hardness, flushing resistance, and controllable morphology, i.e., cerium oxide (CeO_2) was used for polishing along with polydopamine (pDA) as a binder on X80 pipeline steel. Water contact angles of 154.7° and 155.5° were obtained on the CeO_2/pDA@X80 coating in air and cyclopentane, respectively, compared to 82.6° and 84.7° on bare X80 substrate. The water droplet sticks to the metal substrate higher than a 90° tilt angle, while on the prepared surface just at an angle of 3° and 2° in air and CP, respectively, the drop can be rolled off. Mechanical stability of the coating was successfully ascertained through a 2-h-long sand abrasion test. Hydrate adhesion measurements on the coating were done with the help of a micromechanical force apparatus using cyclopentane hydrates before and after the sand abrasion tests. It was reported that the adhesion forces were reduced 98.9% on the superhydrophobic coatings compared to bare steel surface; this ultralow adhesion was maintained even after the sand abrasion tests. The adhesion force between the X80 steel surface and hydrate in the presence of a water droplet was too large to be measured using the micromechanical apparatus. However, the superhydrophobic coating did not allow this situation due to easy detachment of water droplets from it (Figure 3).

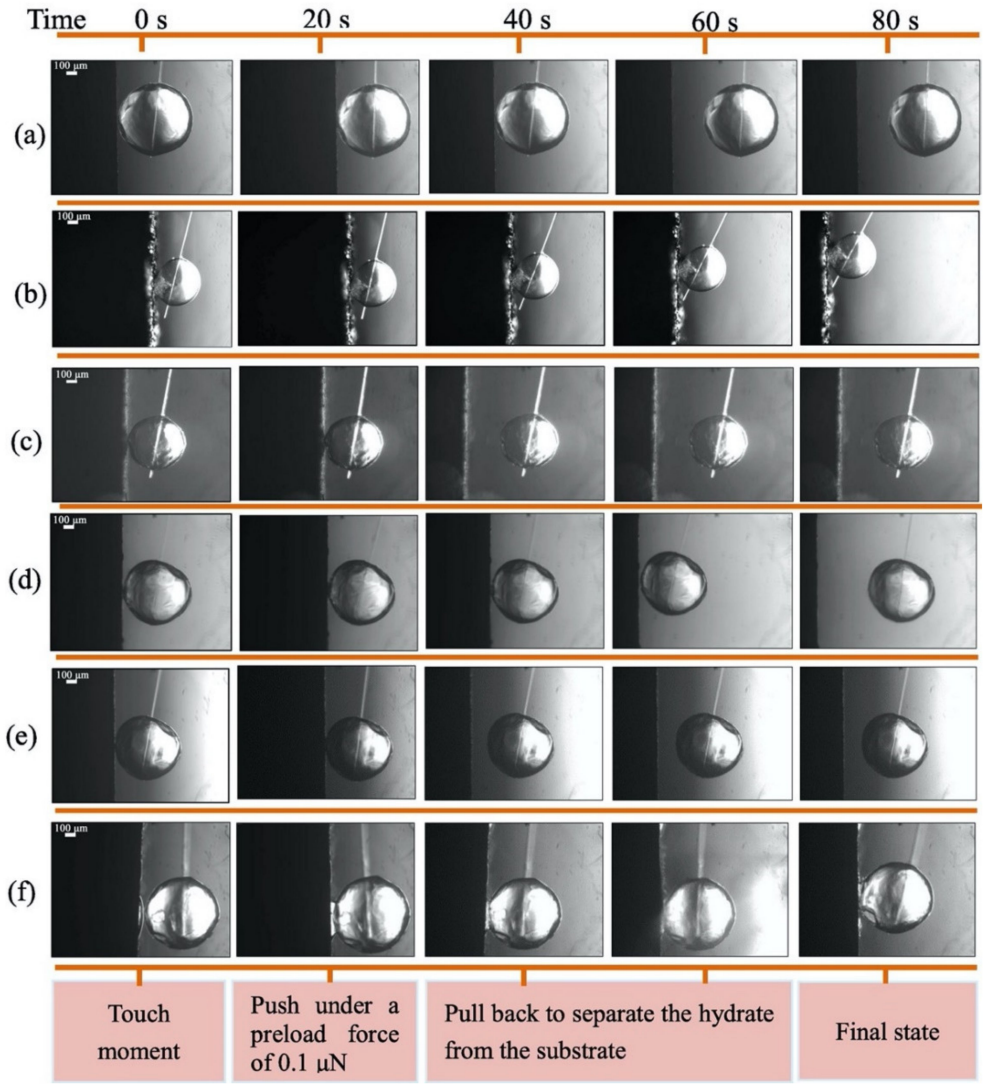

Figure 3. The images obtained at 20-s intervals from the touch moment during the adhesion measurement for different treated substrates: (**a**) X80; (**b**) Coating without surface modification; (**c**) CeO2/pDA@X80 coating; (**d**) X80 after sand abrasion; (**e**) CeO2/pDA@X80 coating after sand abrasion; (**f**) X80 with a water drop deposited on the surface. Reprinted with permission from ref. [54]. © 2021 Elsevier.

3.4. Other Surface Treatments

Recently, Ragunathan et al. [51] demonstrated, as a proof of concept, that a ferrofluid can be used as a coating to create a liquid/liquid interface to reduce the hydrate adhesion on the pipeline walls. This strategy can be applied by pumping the fluid in high-risk areas, namely, a low spot of the tubing and pipeline. The magnets placed on the designated spots of the outer walls, therefore, will assist in the formation of a liquid/liquid interface on the inner wall. The magnetic, slippery surface in this work was prepared by dispersing magnetic particles within a hydrocarbon-based magnetic fluid. The particles were dispersed uniformly in the fluid irrespective of the introduction of a magnetic/force field. The fluid was applied on a metal surface and the adhesion strength of tetrahydrofuran hydrates at atmospheric pressure was measured under static and dynamic conditions. The results indicated that the ferrofluid coating gel did not prevent the ice/hydrate formation but reduced the adhesion strength of both ice/hydrates and reduced the torque values after hydrate formation. As a control, the neodymium magnet coated with diesel oil was used to ensure that the hydrocarbon in the ferrofluid was not responsible for antiadhesion characteristic

of hydrates. The diesel-coated magnet allowed the formation of ice/hydrate. On tilting the magnet at 90°, the ice/hydrate remained stuck to the magnet surface, indicating that the iron particles dispersed in the fluid were mainly responsible for the antiadhesion properties of this formulation. Other mechanical tests were performed on the THF hydrates where the neodymium magnets need to be detached from the hydrate mold by applying some force. In the absence of coating, a significant force was needed, whereas in presence of ferrofluid, a minimum force was needed to overcome the adhesion between magnet and mold. Hydrocarbon-based ferrofluids can be crucial in lowering the production costs because of their low evaporation rate and, therefore, long life. In order to prevent/overcome the depletion of the coating issue over time, a ferrofluid gel was also used. Further tests in realistic, high-pressure conditions are required to fully assess the potential of this strategy. The presence of produced hydrocarbons might dilute the gel/liquid.

Fan et al. [52] pointed out that the surface coatings can significantly reduce the hydrate adhesion strength, which can further be reduced by the application of microscale/nanoscale textures on the surfaces. They chose four different substrates, namely, X70 steel, X80 steel, Zirconia (ZrO_2), and tinplate, which were treated following a rigorous procedure with three different coatings, namely, a fluoro-coating reagent (F-coating), polydimethylsiloxane (PDMS), and hexagonal boron nitride (HBN). Hydrophobic fuming SiO_2 in different proportions was also added in each system to prepare various types of coatings. The sample with 96% PDMS + 4% SiO_2 applied on a bare X70 substrate showed the maximum water contact angle of 158°. A micromechanical force apparatus was used to measure the adhesion forces between the coated surfaces and model hydrate former THF. The results indicated that the combination of coating materials with a specific surface structure applied on an appropriate substrate can lead to reduced adhesion and growth of hydrates. In order to access the efficiency of the coatings to reduce hydrate growth at atmospheric pressure, bare/coated substrates were placed in a cold platform containing THF solutions and the hydrate growth was recorded, and the area calculated using a software (Figure 4). High-pressure experiments with methane as a hydrate former were also carried out in an autoclave to understand the performance and durability of these coatings under field conditions. A steel substrate with one side coated (96% PDMS + 4% SiO_2) and the other uncoated was placed in the autoclave at a 65° angle and partly immersed in the liquid phase. Later, the induction time of the hydrate formation was measured, and it was found that the coated surface delayed the hydrate formation considerably. Moreover, there was no hydrate growth on the coated side, whereas the uncoated side of the substrate was fully covered with hydrate. However, after the high-pressure experiments, the coating immersed inside the liquid phase remained intact, whereas outside the liquid phase got detached, probably due to direct contact with the high-pressure gas phase. Scanning Electron Microscopy was used to obtain the morphologies of bare and coated surfaces and suggested that addition of SiO_2 can alter the surface structure of the coatings. SiO_2 formed a micro-nanostructure that isolated the contacts between hydrate and the coated surfaces, resulting in reduced adhesion and growth of hydrates. The authors concluded that, despite good inhibition performance by PDMS coating, there was still an issue of its stability under a high-pressure environment.

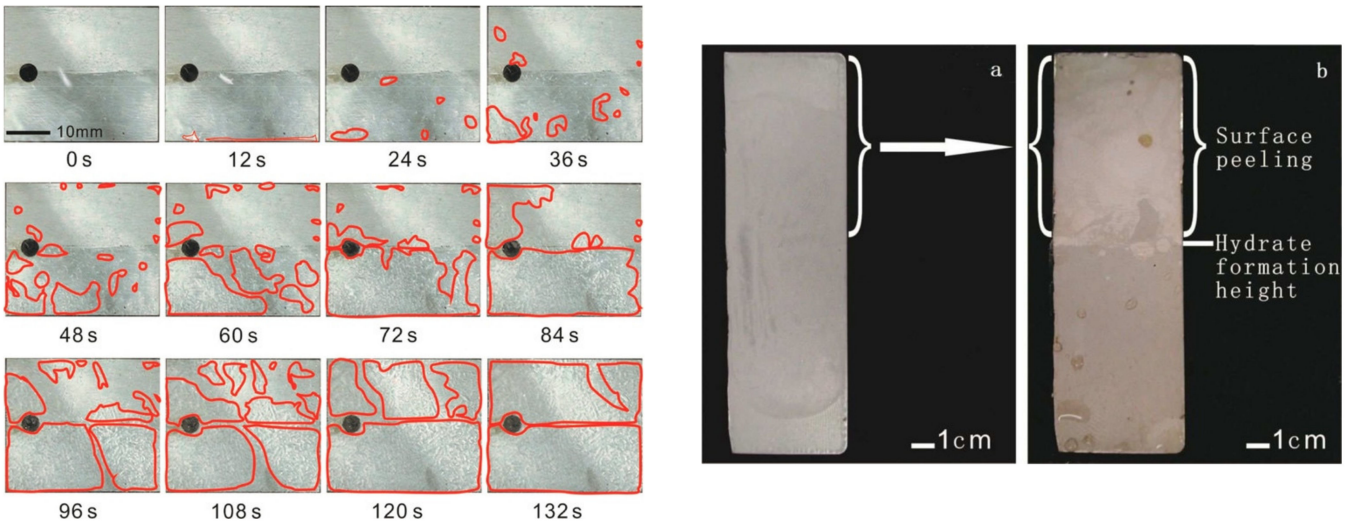

Figure 4. (**Left**) Images depicting THF hydrate growth on coated surfaces over a period of time. (**Right**) The red areas depict the zones where hydrates formed. Changes observed in a coated substrate (**a**) before and (**b**) after the high-pressure methane hydrate formation experiments in an autoclave. Reprinted with permission from ref. [52]. © 2021 American Chemical Society.

4. Surface Active/Hydrate-Philic Coatings

Filasky et al. [55] showed that surface-active coatings produced by silanization can promote the methane hydrate formation. The authors chose glass substrate and silanes of different chain lengths, namely, ethyltriethoxysilane (ES), *n*-dodecyltriethoxysilane (DS), and *n*-octyltriethoxysilane (OE), to create surfaces with varying hydrophobicities that may reduce the surface tension and gas-enriched layer on reactor walls to promote hydrate formation. Later, these silanized surface-active coatings were tested for their influence on the hydrate formation in stationary and dynamic conditions using a high-pressure, stirred autoclave with sight glasses for visual observations. The experiments performed in transient conditions showed almost similar trends on all silanized glasses. However, the results obtained from stationary tests clearly showed a promotion effect. The authors claimed that the distinct experimental setup was the reason for this contrasting behaviour. In stationary tests, methane was injected directly into the hydrate plug using an ascending pipe, which diffused into the methane-saturated layer at the coated-glass surface, resulting in more hydrate formation. This effect was absent during transient experiments because of the presence of a "sealing cork"-like hydrate plug. However, the durability of the coatings under mechanical stress needs to be assessed for their long-term usage.

5. Intellectual Property Generation/Commercialization

A quick search revealed that a few patents have already been granted on this topic, e.g., on the methods to reduce hydrate adhesion [56], hydrophobic surfaces for easy hydrate transportation [57], and a combined surface-chemical approach to inhibit the hydrate deposition [58]. Some commercial products based on polymeric, superhydrophobic, and nanocomposite materials are also available in the market [59–62]. The rapid intellectual property generation and commercialization indicates the potential of coating technology for hydrate management (Figure 5).

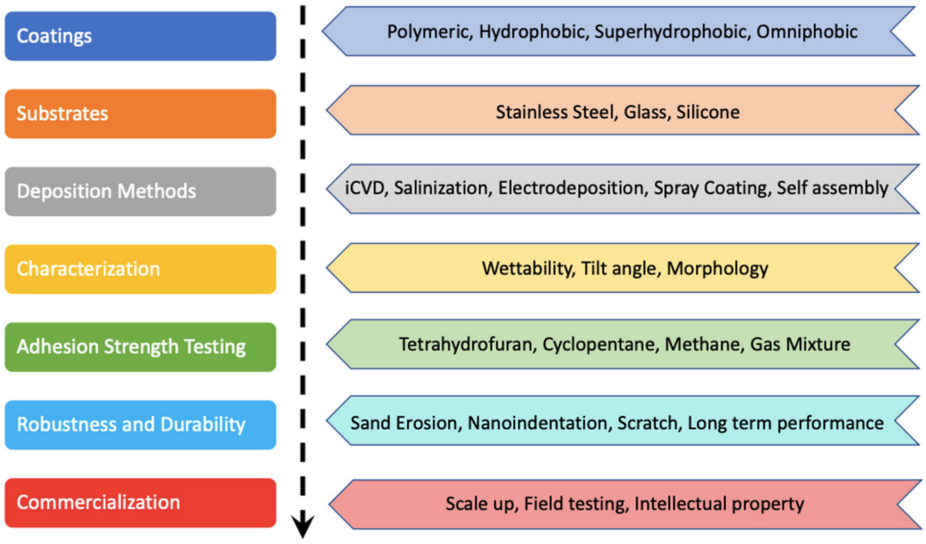

Figure 5. From concept to commercialization: Development stages of an anti-hydrate/hydrate-phobic coating.

6. Conclusions and Future Perspectives

A systematic review of the area of functionalized surface coatings and treatments for controlled hydrate nucleation and growth was presented. The progress made at this front in the last decade was collected and discussed. At this stage, the research focus is shifting towards managing hydrate formation instead of completely avoiding it within the production pipelines. The recent works reported on this topic are more detailed and improve our understanding of the importance of functionalized surfaces as a hydrate management tool (Figure 5). Some important points can be summarized and highlighted from this review:

- Surface chemistry (hydrophobicity/hydrophilicity) and physical state (morphology) are both vital in defining a surface as hydrate-phobic or hydratephilic.
- Hydrate formation is a stochastic process, which depends on various parameters (several repetitions are required to obtain statistically significant results), which also make it impossible to compare the results across laboratories.
- Standard protocols indicating clearly the subcooling temperature, composition of THF/CP hydrate forming solutions, and parameters to assess the performance of a coating should be established for round robin measurements so that the results from different laboratories can be compared.
- The results obtained for THF/CP (type sII) model hydrates at atmospheric pressure should only be made with gaseous hydrates that form a similar hydrate structure at high pressure.
- In the future, screening of more robust and environmentally benign surface treatments/coatings, which are economic, can be prepared rapidly at large scale, and be multi-functional in nature, needs to be assessed.
- Systematic molecular modelling studies need to be pursued to unravel the mechanism by which a given surface alters the hydrate adhesion.

The area of hydrate-promoting functionalized surfaces that can accelerate the rate of hydrate formation and growth is relatively unexplored. Progress at this front will immensely improve various applications based on hydrate technology for energy- and environment-related purposes. We believe that the coming decade will see a surge in research activities in this area.

Author Contributions: Conceptualization, M.T., T.A.; Writing–original draft preparation, T.A.; Writing–review and editing, M.T., J.M.S.S.E.; Fund acquisition, M.T. and J.M.S.S.E. All authors have read and agreed to the published version of the manuscript.

Funding: This work was supported by the Associate Laboratory for Green Chemistry-LAQV, which is financed by national funds from Fundação para a Ciência e Tecnologia, FCT/MCTES (UIDB/50006/2020, UIDP/50006/2020, and LA/P/0008/2020). The support through project PTDC/EQU-EQU/32050/2017, funded by Fundação para a Ciência e Tecnologia, FCT/MCTES (Portugal), is also acknowledged.

Institutional Review Board Statement: Not applicable.

Informed Consent Statement: Not applicable.

Data Availability Statement: Not applicable.

Conflicts of Interest: The authors declare no conflict of interest.

References

1. Sloan, E.D.; Koh, C.A. *Clathrate Hydrates of Natural Gases*, 3rd ed.; CRC Press: Boca Raton, FL, USA, 2008; Volume 119, pp. 1–752.
2. Koh, C.A.; Sloan, E.D.; Sum, A.K.; Wu, D.T. Fundamentals and Applications of Gas Hydrates. *Annu. Rev. Chem. Biomol. Eng.* **2011**, *2*, 237–257. [CrossRef] [PubMed]
3. Hassanpouryouzband, A.; Joonaki, E.; Farahani, M.V.; Takeya, S.; Ruppel, C.; Yang, J.; English, N.J.; Schicks, J.M.; Edlmann, K.; Mehrabian, H.; et al. Gas hydrates in sustainable chemistry. *Chem. Soc. Rev.* **2020**, *49*, 5225–5309. [CrossRef] [PubMed]
4. Ripmeester, J.A.; Alavi, S. Some current challenges in clathrate hydrate science: Nucleation, decomposition and the memory effect. *Curr. Opin. Solid State Mater. Sci.* **2016**, *20*, 344–351. [CrossRef]
5. Sloan, E.D. Gas hydrates: Review of physical/chemical properties. *Energy Fuels* **1998**, *12*, 191–196. [CrossRef]
6. Sum, A.K.; Koh, C.A.; Sloan, E.D. Developing a comprehensive understanding and model of hydrate in multiphase flow: From laboratory measurements to field applications. *Energy Fuels* **2012**, *26*, 4046–4052. [CrossRef]
7. Creek, J.L. Efficient Hydrate Plug Prevention. *Energy Fuels* **2012**, *26*, 4112–4116. [CrossRef]
8. Kinnari, K.; Hundseid, J.; Li, X.; Askvik, K.M. Hydrate management in practice. *J. Chem. Eng. Data* **2015**, *60*, 437–446. [CrossRef]
9. Metaxas, P.J.; Lim, V.W.S.; McKay, S.F.; Morgan, J.E.P.; Johns, M.L.; Aman, Z.M.; May, E.F. High-fidelity evaluation of hybrid gas hydrate inhibition strategies. *Energy Fuels* **2012**, *34*, 15893–15989. [CrossRef]
10. Song, S.; Shi, B.; Yu, W.; Ding, L.; Liu, Y.; Li, W.; Gong, J. Study on the optimization of hydrate management strategies in deepwater gas well testing operations. *J. Energy Resour. Technol.* **2020**, *142*, 033002. [CrossRef]
11. Kelland, M.A. History of the development of low dosage hydrate inhibitors. *Energy Fuels* **2006**, *20*, 825–847. [CrossRef]
12. Tohidi, B.; Anderson, R.; Mozaffar, H.; Tohidi, F. The return of kinetic hydrate inhibitors. *Energy Fuels* **2015**, *29*, 8254–8260. [CrossRef]
13. Khurana, M.; Yin, Z.; Linga, P. A review of clathrate hydrate nucleation. *ACS Sustain. Chem. Eng.* **2017**, *5*, 11176–11203. [CrossRef]
14. Yin, Z.; Khurana, M.; Tan, H.K.; Linga, P. A review of gas hydrate growth kinetic models. *Chem. Eng. J.* **2018**, *342*, 9–29. [CrossRef]
15. Zerpa, L.E.; Salager, J.-L.; Koh, C.A.; Sloan, E.D.; Sum, A.K. Surface chemistry and gas hydrates in flow assurance. *Ind. Eng. Chem. Res.* **2011**, *50*, 188–197. [CrossRef]
16. Giavarini, C.; Hester, K. *Gas Hydrate: Immense Energy Potential and Environmental Challenges*, 1st ed.; Springer: London, UK, 2011; pp. 1–178.
17. Eslamimanesh, A.; Mohammadi, A.H.; Richon, D.; Naidoo, P.; Ramjugernath, D. Application of gas hydrate formation in separation processes: A review of experimental studies. *J. Chem. Thermodyn.* **2012**, *46*, 62–71. [CrossRef]
18. Sabil, K.M.; Partoon, B. Recent advances on carbon dioxide capture through a hydrate-based gas separation process. *Curr. Opin. Green Sustain. Chem.* **2018**, *11*, 22–26. [CrossRef]
19. Veluswamy, H.P.; Kumar, A.; Seo, Y.; Lee, J.D.; Linga, P. A review of solidified natural gas (SNG) technology for gas storage via clathrate hydrates. *Appl. Energy* **2018**, *216*, 262–285. [CrossRef]
20. Straume, E.O.; Morales, R.E.M.; Sum, A.K. Perspectives on gas hydrates cold flow technology. *Energy Fuels* **2019**, *33*, 1–15. [CrossRef]
21. Zheng, J.; Chong, Z.R.; Qureshi, M.F.; Linga, P. Carbon dioxide sequestration via gas hydrates: A potential pathway toward decarbonization. *Energy Fuels* **2020**, *34*, 10529–10546. [CrossRef]
22. Babu, P.; Nambiar, A.; He, T.; Karimi, I.A.; Lee, J.D.; Englezos, P.; Linga, P. A Review of clathrate hydrate based desalination to strengthen energy–water nexus. *ACS Sustain. Chem. Eng.* **2018**, *6*, 8093–8107. [CrossRef]
23. Kumar, A.; Bhattacharjee, G.; Kulkarni, B.D.; Kumar, R. Role of surfactants in promoting gas hydrate formation. *Ind. Eng. Chem. Res.* **2019**, *54*, 12217–12232. [CrossRef]
24. Linga, P.; Clarke, M.A. A review of reactor design and materials employed for increasing the rate of gas hydrate formation. *Energy Fuels* **2017**, *31*, 1–12. [CrossRef]
25. Nashed, O.; Partoon, B.; Lal, B.; Sabil, K.M.; Shariff, A.M. Review the impact of nanoparticles on the thermodynamics and kinetics of gas hydrate formation. *J. Nat. Gas Sci. Eng.* **2015**, *55*, 452–465. [CrossRef]

26. Song, Y.M.; Liang, R.-Q.; Wang, F.; Shi, J.-H.; Zhang, D.-B.; Yang, L. Enhancement of clathrate hydrate formation kinetics using carbon-based material promotion. *Front. Chem.* **2020**, *8*, 464. [CrossRef]
27. Liu, N.; Chen, L.; Liu, C.; Yang, L.; Liu, D. Experimental study of carbon dioxide hydrate formation in the presence of graphene oxide. *Energy* **2020**, *211*, 118994. [CrossRef]
28. Zhang, G.; Shi, X.; Zhang, R.; Chao, K.; Wang, F. Promotion of activated carbon on the nucleation and growth kinetics of methane hydrates. *Front. Chem.* **2020**, *8*, 526101. [CrossRef]
29. Hu, P.; Chen, D.; Zi, M.; Wu, G. Effects of carbon steel corrosion on the methane hydrate formation and dissociation. *Fuel* **2018**, *230*, 126–133. [CrossRef]
30. Hu, P.; Wu, G.; Zi, M.; Li, L.; Chen, D. Effects of modified metal surface on the formation of methane hydrates. *Fuel* **2019**, *255*, 115720. [CrossRef]
31. Chenwei, L.; Zhiyuan, W.; Jinlin, T.; Ci, Y.; Mingzhong, L. Fundamental investigation of the adhesion strength between cyclopentane hydrate deposition and solid surface materials. *Chem. Eng. Sci.* **2020**, *217*, 115524. [CrossRef]
32. Esmail, S.; Beltran, J.G. Methane hydrate propagation on surfaces of varying wettability. *J. Nat. Gas Sci. Eng.* **2016**, *35*, 1535–1543. [CrossRef]
33. Beltran, J.G.; Servio, P. Morphological investigations of methane-hydrate films formed on a glass surface. *Cryst. Growth Des.* **2010**, *10*, 4339–4347. [CrossRef]
34. Li, H.; Wang, L. Hydrophobized particles can accelerate nucleation of clathrate hydrates. *Fuel* **2015**, *140*, 440–445. [CrossRef]
35. Acharya, P.V.; Kar, A.; Shahriari, A.; Bhati, A.; Mhadeshwar, A.; Bahadur, V. Aluminium-base promotion of nucleation of carbon dioxide hydrates. *J. Phys. Chem. Lett.* **2020**, *11*, 1477–1482. [CrossRef] [PubMed]
36. Kar, A.; Acharya, P.V.; Bhati, A.; Mhadeshwar, A.; Venkataraman, P.; Barckholtz, T.A.; Celio, H.; Mangolini, F.; Bahadur, V. Magnesium-promoted rapid nucleation of carbon dioxide hydrates. *ACS Sustain. Chem. Eng.* **2021**, *9*, 11137–11146. [CrossRef]
37. Nguyen, N.N.; Galib, M.; Nguyen, A.V. Critical review on gas hydrate formation at solid surfaces and in confined spaces—Why and how does interfacial regime matter? *Energy Fuels* **2020**, *34*, 6751–6760. [CrossRef]
38. Wang, Y.; Fan, S.; Lang, X. Reviews of gas hydrate inhibitors in gas-dominant pipelines and application of kinetic hydrate inhibitors in China. *Chin. J. Chem. Eng.* **2019**, *27*, 2118–2132. [CrossRef]
39. Manakov, A.Y.; Penkov, N.V.; Rodionova, T.V.; Nesterov, A.N.; Fesenko, E.F., Jr. Kinetics of formation and dissociation of gas hydrates. *Russ. Chem. Rev.* **2017**, *86*, 845–869. [CrossRef]
40. Smith, J.D.; Meuler, A.J.; Bralower, H.; Venkatesan, R.; Subramanian, S.; Cohen, R.E.; McKinley, G.H.; Varanasi, K.K. Hydrate-phobic surfaces: Fundamental studies in clathrate hydrate adhesion reduction. *Phys. Chem. Chem. Phys.* **2012**, *14*, 6013–6020. [CrossRef] [PubMed]
41. Aman, Z.M.; Sloan, E.D.; Sum, A.K.; Koh, C.A. Adhesion force interactions between cyclopentane hydrate and physically and chemically modified surfaces. *Phys. Chem. Chem. Phys.* **2014**, *16*, 25121–25128. [CrossRef] [PubMed]
42. Sojoudi, H.; Walsh, M.R.; Gleason, K.K.; McKinley, G.H. Designing durable vapor-deposited surfaces for reduced hydrate adhesion. *Adv. Mat. Interfaces* **2015**, *2*, 1500003–1500015. [CrossRef]
43. Sojoudi, H.; Walsh, M.R.; Gleason, K.K.; McKinley, G.H. Investigation into the formation and adhesion of cyclopentane hydrates on mechanically robust vapor-deposited polymeric coatings. *Langmuir* **2015**, *31*, 6186–6196. [CrossRef] [PubMed]
44. Perfeldt, C.M.; Sharifi, H.; von Solms, N.; Englezos, P. Oil and gas pipelines with hydrophobic surfaces better equipped to deal with gas hydrate flow assurance issues. *J. Nat. Gas Sci. Eng.* **2015**, *27*, 852–861. [CrossRef]
45. Hall, J.R.; Baures, P.W. Inhibition of tetrahydrofuran hydrate formation in the presence of polyol-modified glass surfaces. *Energy Fuels* **2017**, *31*, 7816–7823. [CrossRef]
46. Das, A.; Farnham, T.A.; Subramanyam, S.B.; Varanasi, K.K. Designing ultra-low hydrate adhesion surfaces by interfacial spreading of water immiscible barrier films. *ACS Appl. Mater. Interfaces* **2017**, *9*, 21496–21502. [CrossRef]
47. Brown, E.; Hu, S.; Wang, S.; Wells, J.; Nakatsuka, M.; Veedu, V.; Koh, C.A. Low-adhesion coatings as a novel gas hydrate mitigation strategy. In Proceedings of the Offshore Technology Conference, Houston, TX, USA, 1–4 May 2017.
48. Di Lullo, A.; Zonta, P.P.; Pontarollo, A.; Correra, S. Measurment of adhesion strength of methane hydrates to wall. *Recent Adv. Petrochem. Sci.* **2018**, *4*, 59–61. [CrossRef]
49. Sojoudi, H.; Arabnejad, H.; Raiyan, A.; Shirazi, S.A.; McKinley, G.H.; Gleason, K.K. Scalable and durable polymeric icephobic and hydrate-phobic coatings. *Soft Matter* **2018**, *14*, 3443. [CrossRef]
50. Pickarts, M.A.; Brown, E.; Delgado-Linares, J.; Blanchard, G.; Veedu, V.; Koh, C.A. Deposition mitigation in flowing systems using coatings. In Proceedings of the Offshore Technology Conference, Houston, TX, USA, 6–9 May 2019.
51. Ragunathan, T.; Xu, X.; Shuhili, J.A.; Wood, C.D. Preventing hydrate adhesion with magnetic slippery surfaces. *ACS Omega* **2019**, *4*, 15789–15797. [CrossRef]
52. Fan, S.; Zhang, H.; Yang, G.; Wang, Y.; Li, G.; Lang, X. Reduction clathrate hydrates growth rates and adhesion forces on surfaces of inorganic or polymer coatings. *Energy Fuels* **2020**, *34*, 13566–13579. [CrossRef]
53. Dong, S.; Li, M.; Liu, C.; Zhang, J.; Chen, G. Bio-inspired superhydrophobic coating with low hydrate adhesion for hydrate mitigation. *J. Bionic Eng.* **2020**, *17*, 1019–1028. [CrossRef]
54. Zhang, W.; Fan, S.; Wang, Y.; Lang, X.; Li, G. Preparation and performance of biomimetic superhydrophobic coating on X80 pipeline steel for inhibition of hydrate adhesion. *Chem. Eng. J.* **2021**, *419*, 129651. [CrossRef]

55. Filarsky, F.; Schmuck, C.; Schultz, H.J. Development of a surface-active coating for promoted gas hydrate formation. *Chem. Ing. Tech.* **2019**, *91*, 85–91. [CrossRef]
56. Smith, J.D.; Varanasi, K.K.; McKinley, G.H.; Cohen, R.E.; Meuler, A.J.; Bralower, H.L. Massachusetts Institute of Technology, Articles and Methods for Reducing Hydrate Adhesion. U.S. Patent US2012/0160362A1, 28 June 2012.
57. Hatton, G.J.; Mehta, A.P.; Peters, D.J. Pipe Transportation System with Hydrophobic Wall. Chinese Patent CN102959301B, 19 August 2015. U.S. Patent US2013/0087207A1, 11 April 2013.
58. Bhatnagar, G.; Crosby, D.L.; Hatton, G.J.; Huo, Z.; Shell Internationale Research Maatschappij B., V. Hydrate deposit inhibition with surface-chemical combination. World Patent WO2012/058144A3, 3 May 2012.
59. DragX Flow Assurance & Efficiency Home Page. Available online: https://dragxsurfaces.com (accessed on 2 December 2021).
60. Southwest Research Institute Press Releases Page. Available online: https://www.swri.org/press-release/superhydrophobic-coating-process-subsea-pipelines (accessed on 2 December 2021).
61. DuBose, B. Materials Performance Coatings and Linings Section. Available online: https://www.materialsperformance.com/articles/coating-linings/2020/03/superhydrophobic-coating-developed-for-offshore-drilling-pipes (accessed on 2 December 2021).
62. Evonik Products and Solutions Page. Available online: https://corporate.evonik.com/en/products/industry-teams/oil-gas/products-markets/flowlines-and-pipelines-123783.html (accessed on 2 December 2021).
63. Lingelem, M.N.; Majeed, A.I.; Stange, E. Industrial experience in evaluation of hydrate formation, inhibition, and dissociation in pipeline design and operation. *Ann. N. Y. Acad. Sci.* **1994**, *715*, 75–93. [CrossRef]
64. Austvik, T.; Li, X.; Gjertsen, L.H. Hydrate plug properties: Formation and removal of plugs. *Ann. N. Y. Acad. Sci.* **2000**, *912*, 294–303. [CrossRef]
65. Nicholas, J.W.; Dieker, L.E.; Sloan, E.D.; Koh, C.A. Assessing the feasibility of hydrate deposition on pipeline walls–adhesion force measurements of clathrate hydrate particle on carbon steel. *J. Colloid Interface Sci.* **2009**, *331*, 322–328. [CrossRef] [PubMed]
66. Aspenes, G.; Dieker, L.E.; Aman, Z.M.; Hoiland, S.; Sum, A.K.; Koh, C.A.; Sloan, E.D. Adhesion force between cyclopentane hydrates and solid surface materials. *J. Colloid Interface Sci.* **2010**, *343*, 529–536. [CrossRef] [PubMed]
67. Liu, C.; Li, M.; Zhang, G.; Koh, C.A. Direct measurements of the interactions between clathrate hydrate particles and water droplets. *Phys. Chem. Chem. Phys.* **2015**, *17*, 20021–20029. [CrossRef] [PubMed]
68. Aman, Z.M.; Joshi, S.E.; Sloan, E.D.; Sum, A.K.; Koh, C.A. Micromechanical cohesion force measurements to determine cyclopentane hydrate interfacial properties. *J. Colloid Interface Sci.* **2012**, *376*, 283–288. [CrossRef]
69. Aman, Z.M.; Koh, C.A. Interfacial phenomena in gas hydrate systems. *Chem. Soc. Rev.* **2016**, *45*, 1678–1690. [CrossRef] [PubMed]
70. Grasso, G.A.; Vijayamohan, P.; Sloan, E.D.; Koh, C.A.; Sum, A.K. Gas hydrate deposition in flowlines: A challenging problem in flow assurance. In Proceedings of the ASME, 32nd International Conference Ocean, Offshore and Arctic Engineering, Nantes, France, 9–14 June 2013.